A THERMODYNAMICALLY BASED WORK POTENTIAL THEORY FOR PREDICTING PROGRESSIVE DAMAGE AND FAILURE IN 3D TEXTILE COMPOSITES

H. Sam Huang[1], Evan J. Pineda[2]

[1]Department of Mechanical Engineering, State University of New York, Stony Brook, New York, USA
Email: sam.huang@stonybrook.edu
[2]Multiscale and Multiphysics Modeling Branch, NASA Glenn Research Center Cleveland, OH , USA
Email: evan.j.pineda@nasa.gov

Keywords: Textile composites 1, finite element analysis 2, progressive failure 3, thermodynamics 4,

Abstract

In this paper, a 3D thermodynamically-based work potential theory for modeling progressive damage for laminated, unidirectional composites,extend from 2D Schapery's theory, is used to predict the response of unidirectional composites under three point bending. An internal state variable, S, is defined to account for the dissipated energy due to damage evolution in the form of microstructural changes in the matrix. With the stationary of the total work potential with respect to the internal state variable, a thermodynamically-consistent set of evolution equations is derived. The internal state variable is related to the transverse and shear moduli through microdamage functions. The shear modulus and transverse modulus expressed as a function of internal state variable are obtained from coupon tests. The shear modulus and transverse modulus expressed as a function of internal state variable are implemented into 3D Schaperys theory to predict unidirectional composites under three point bending. The comparison of show good agreement between simulations and experiments under three point bending.

1. Introduction

Development of reliable computational methods for the prediction of laminated progressive failure has advanced for decades and is an ongoing active research effort. Damage simulations in composites can be broadly divided into four categories. The first category is based on the first-ply failure criteria approach [1] which was initially developed for lamina in unidirectional composites. The disadvantage in using the first-ply failure criteria approach is that, once a failure criterion is met, the whole lamia is regarded as have failed. Neither the position, or evolution, of damage or crack can be predicted, which often leads to error in the structural failure predictions. The second approach is based on fracture mechanics where the energy release rate, defined as energy dissipated during fracture per unit of created fracture surface area, is compared against a critical energy release rate to determine whether cracks advance [2]. The third approach uses plasticity which is more appropriate for composites exhibiting ductile behavior [3], although substantial permanent deformation may not exist upon unloading of the composite. The fourth approach is progressive failure modeling based on the continuum damage mechanics (CDM) approach [4] [5] [6] [7] [8]. The advantage of the CDM approach is that it can use stress and or strain failure criteria for predicting damage initiation coupled with progressive failure evolution.

Over the past two decades, polymer textile fiber composites (TFCs) have become attractive for lightweight applications because of their inherent toughness and inexpensive manufacturing costs. Detailed intro-

Excerpt from ISBN 978-3-00-053387-7

duction to TFCs can be seen in [9] and [10]. Laminated textile composites have been used in adaptive wind turbine blades [11] and in the automobile [12]. Textile fiber composites are flexible. In that, the microstructure can be tailored to attain the desired, macroscopic mechanical properties.

In order to reliably and accurately predict progressive failure of textile composites, it is necessary to develop a mesoscale model in which the morphology of the fiber tows is captured by explicitly modeling the weave architecture. However, from the hierarchical structure of textile composites, shown in Figure 1, it can be seen that the fiber tows locally can be treated as transversely isotropic materials. One strategy for modeling TFCs is to employ the same methods used for unidirectional composites within the fiber tows of a mesoscale model [13] [14]. Moreover, the plane stress assumption often used for unidirectional laminates does not hold locally for the fiber tows because of the tow undulations and weave architecture. Thus, a 3D, transversely isotropic, constitutive model must be developed, and understanding the progressive failure of unidirectional laminates is the first step towards modeling the progressive failure of textile composites.

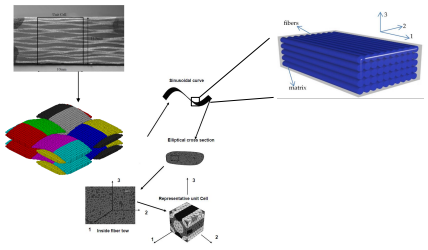

Figure 1. Hierarchical structures of textile composites.

Schapery proposed a thermodynamically based work potential theory for progressive failure of unidirectional composites [15]. The cited formulation utilizes a plane stress assumption for laminated plates. In Schapery's theory, the response in the fiber direction is linear, whereas damage due to microscopic cracking in the matrix affects the transverse modulus and shear modulus. Thus, the instantaneous transverse and shear moduli are functions of damage, represented with an internal state variable, accumulated during the loading. Schaperys theory has previously been implemented within the finite element method to model the tensile and compressive response of 2D, notched composite plates [7] [8].

In this paper, the plane stress formulation of Schapery's theory [15] for laminates is extended to accommodate a fully 3D stress state while maintaining the transversely isotropic assumption commonly used for unidirectional composites. The 3D theory is implemented within the Abaqus finite element method software package via a user defined subroutine (UMAT). This numerical implementation is used to model unidirectional laminates with the intent of using it in the future for modeling progressive failure of the fiber tows in TFCs. A crux of Schaperys theory is the use of microdamage functions, obtained from coupon experiments, to relate the degraded stiffnesses to the internal state variable. There exists a great amount of flexibility in how the experimental data is fit to obtain the microdamage functions. Sicking [16] observed that the internal state variable S, which represents the matrix microdamage evolves as the cube of the applied strain. Thus, Sicking introduced a reduced internal state variable S_r, defined as $S^{\frac{1}{3}}$. Subsequently, the Young's modulus and shear modulus were defined as polynomial functions in S_r. An additional focus of the present work is to analyze and compare progressive failure predictions obtained using various forms of the matrix microdamage functions. Three different forms for the matrix microdamage functions, where the exponent that defines the reduced internal state variable and the order

Excerpt from ISBN 978-3-00-053387-7

of the polynomial fit of the stiffness versus reduced internal state variable data are varied, are used as input in Schapery's theory. A notched composites panel is created to conduct compression simulations using the three methods. Finally, the results are compared and summary are presented.

2. Guidelines

3. 3D formulation of Schapery's theory for unidirectional composites

Schapery proposed a thermodynamically-based work potential theory for laminated composites[15]. Over the years, the theory has been used and extended by different researchers [8],[7], [6] to model progressive failure of laminated composites within the finite element method. An internal state variable, S, is used to describe the energy dissipated in Figure 2 due to damage or microstructural changes under loading. From experiment, it has been shown that there is negligible stiffness degradation in the longitudinal (or fiber) direction but stiffness degradation, due to damage accumulation, does occur in the transverse direction. Thus, the transverse and shear stiffnesses are not constant but are functions of the internal state of the material.

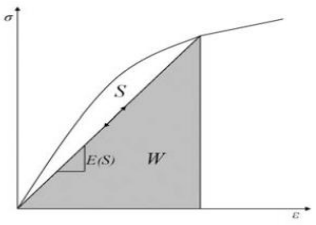

Figure 2. Schematic of state variable S and recoverable energy density W [6]

The total work potential, W_T , is the sum of the recoverable, elastic strain energy density, W_{Strain}, and the dissipated energy potential, S.

$$W_T = W_{Strain} + S \tag{1}$$

Due to the principle of stationarity of the total work potential with respect to the internal state variable, at any instant of thermodynamic equilibrium, the following equation holds

$$\frac{\partial W_T}{\partial S} = 0 \tag{2}$$

Also, the dissipated energy ,S, is not reversible. That is,

$$\dot{S} \geq 0 \tag{3}$$

Substituting Eq (1) into Eq (2), the evolution equation for laminated composites can be derived.

Assuming the local coordinate 1 is defined to align with the fiber direction, direction 2 and direction 3 are aligned with the transverse direction normal to the fiber direction. The fully 3D strain state can be

Excerpt from ISBN 978-3-00-053387-7

expressed in terms of stress by the compliance matrix, $[C]$. That is , $\{\varepsilon\}= [C]\ \{\sigma\}$ where $[C]$ is expressed as follows

$$[C] = \begin{bmatrix} \frac{1}{E_1} & \frac{-\nu_{21}}{E_2} & \frac{-\nu_{21}}{E_2} & 0 & 0 & 0 \\ \frac{-\nu_{12}}{E_1} & \frac{1}{E_2} & \frac{-\nu_{23}}{E_2} & 0 & 0 & 0 \\ \frac{-\nu_{12}}{E_1} & \frac{-\nu_{23}}{E_2} & \frac{1}{E_2} & 0 & 0 & 0 \\ 0 & 0 & 0 & \frac{(1+\nu_{23})}{E_2} & 0 & 0 \\ 0 & 0 & 0 & 0 & \frac{1}{2G_{12}} & 0 \\ 0 & 0 & 0 & 0 & 0 & \frac{1}{2G_{12}} \end{bmatrix} \tag{4}$$

The five parameters, $E_1, E_2, G_{12}, \nu_{21}, \nu_{23}$ are used to describe a transversely isotropic lamina, or fiber tow. Due to symmetry, the term $\frac{-\nu_{21}}{E_2}$ is equivalent to the term $\frac{-\nu_{12}}{E_1}$. Thus, ν_{12} is not an independent variable. By taking the inverse of the compliance matrix [C], the stiffness matrix [K] can be expressed as the following

$$\begin{bmatrix} K_{11} & K_{12} & K_{12} & 0 & 0 & 0 \\ K_{12} & K_{22} & K_{23} & 0 & 0 & 0 \\ K_{12} & K_{23} & K_{22} & 0 & 0 & 0 \\ 0 & 0 & 0 & K_{44} & 0 & 0 \\ 0 & 0 & 0 & 0 & K_{55} & 0 \\ 0 & 0 & 0 & 0 & 0 & K_{55} \end{bmatrix} \tag{5}$$

where

$$K_{11} = \frac{E_1 E_2(-1+\nu_{23})}{2E_1\nu_{21}^2 + E_2(-1+\nu_{23})} \tag{6}$$

$$K_{12} = \frac{-E_1 E_2 \nu_{21}}{2E_1\nu_{21}^2 + E_2(-1+\nu_{23})} \tag{7}$$

$$K_{22} = \frac{-E_2(E_2 - E_1\nu_{21}^2)}{(2E_1\nu_{21}^2 + E_2(-1+\nu_{23}))(1+\nu_{23})} \tag{8}$$

$$K_{23} = \frac{-E_2(E_2\nu_{23} + E_1\nu_{21}^2)}{(2E_1\nu_{21}^2 + E_2(-1+\nu_{23}))(1+\nu_{23})} \tag{9}$$

$$K_{44} = \frac{E_2}{(1+\nu_{23})} \tag{10}$$

Excerpt from ISBN 978-3-00-053387-7

$$K_{55} = 2G_{12} \tag{11}$$

Typically, the product of two Poisson ratios is relatively small; i.e., $\nu_{21}\nu_{21} << 1$. Thus, [K] matrix can be simplified as the following

$$[K] = \begin{bmatrix} E_1 & \frac{E_1\nu_{21}}{1-\nu_{23}} & \frac{E_1\nu_{21}}{1-\nu_{23}} & 0 & 0 & 0 \\ \frac{E_1\nu_{21}}{1-\nu_{23}} & E_2 & E_2\nu_{23} & 0 & 0 & 0 \\ \frac{E_1\nu_{21}}{1-\nu_{23}} & E_2\nu_{23} & E_2 & 0 & 0 & 0 \\ 0 & 0 & 0 & \frac{E_2}{(1+\nu_{23})} & 0 & 0 \\ 0 & 0 & 0 & 0 & 2G_{12} & 0 \\ 0 & 0 & 0 & 0 & 0 & 2G_{12} \end{bmatrix} \tag{12}$$

Expanding the elastic strain energy density $W_{strain} = \frac{\{\varepsilon\}^T[K]\{\varepsilon\}}{2}$ by use of Eq (12), one can obtain

$$\begin{aligned} W_{strain} = \tfrac{1}{2}(&G_{12}(S)\gamma_{12}^2 + E_2(S)\varepsilon_{22}^2 \\ &+ G_{12}(S)\gamma_{31}^2 + E_2(S)\varepsilon_{33}^2 + \tfrac{2E_1\varepsilon_{22}\varepsilon_{11}\nu_{23}}{1-\nu_{23}} + \tfrac{2E_1\varepsilon_{33}\varepsilon_{11}\nu_{23}}{1-\nu_{23}} \\ &+ \tfrac{E_1\varepsilon_{11}^2}{1-\nu_{23}} + 2E_2(S)\varepsilon_{22}\varepsilon_{33}\nu_{23} - \tfrac{E_1\varepsilon_{11}^2\nu_{23}}{1-\nu_{23}} + \tfrac{E_2(S)\gamma_{23}^2}{2(1+\nu_{23})}) \end{aligned} \tag{13}$$

Where $\gamma_{ij} = 2\varepsilon_{ij}$ are the engineering (as opposed to tensorial) definitions of shear strain. Note that, only the transverse Young's modulus, E_2, and shear modulus, G_{12}, are functions of S, per the previously stated assumptions about the matrix damage modes. The damage moduli are related to the virgin (undamaged) moduli E_{20} and G_{120} and the internal state variable S through a pair of matrix microdamage functions e_s and g_s that are obtained from three coupon experiments.

$$E_2 = E_{20}e_s(S) \tag{14}$$

$$G_{12} = G_{120}g_s(S) \tag{15}$$

The components of the stiffness matrix $K_{22} = K_{33}$ and $K_{55} = K_{66}$ for all S so the stiffness matrix remains transversely isotropic even as damage evolves. This type of damage evolution mimics a spherical type of damage growth, although E_{11} is assumed unaffected due because of the presence of the fiber, rather than planar cracks. This assumption was used to simplify the formulation and implementation of this damage model by eliminating the requirement of defining a crack orientation in 3D space.

Substituting Eq. (13) and Eq. (1) into Eq (2) results in an evolution equation that can be used to solve for S for a given strain state. Following [15] a reduced internal state variable S_r can be used in place of S, so that the experimental data can be easily fit with a polynomial

$$S_r = S^{\frac{1}{n}} \tag{16}$$

Excerpt from ISBN 978-3-00-053387-7

With Eq (16) and the chain rule for derivatives, Eq (2) can be written as follows

$$\frac{\partial W_{strain}}{\partial S_r} = -nS_r^{n-1} \tag{17}$$

In the literature [15] [6] [8], both E_2 and G_{12} are expressed by 5th order polynomial of S_r.

Different combinations of orders of polynomials for E_2 and G_{12} and objectivity are studied in [17]. In this section, derivation with regard to 5th order polynomial for E_2 and 5th order polynomial for G_{12} are presented in the following.

$$E_2 = E_{20}(e_0 + e_1 S_r + e_2 S_r^2 + e_3 S_r^3 + e_4 S_r^4 + e_5 S_r^5) \tag{18}$$

$$G_{12} = G_{120}(g_0 + g_1 S_r + g_2 S_r^2 + g_3 S_r^3 + g_4 S_r^4 + g_5 S_r^5) \tag{19}$$

Substituting Eq (18) and Eq (19), Eq (13) into the evolution equation Eq (17), one can obtain the evolution equation in terms of a fifth order polynomial for S_r expressed as the following

$$a_0 + a_1 S_r + a_2 S_r^2 + a_3 S_r^3 + a_4 S_r^4 = 0 \tag{20}$$

where

$$a_0 = \frac{g_1 G_{120}(\gamma_{12}^2 + \gamma_{31}^2)}{2} + \frac{e_1 E_{20}(\gamma_{23}^2)}{4} + \frac{e_1 E_{20}(\varepsilon_{22}^2 + \varepsilon_{33}^2)}{2} + e_1 E_{20}\varepsilon_{22}\varepsilon_{33}\nu_{23} \tag{21}$$

$$a_1 = g_2 G_{120}(\gamma_{12}^2 + \gamma_{31}^2) + e_2 E_{20} (\varepsilon_{22}^2 + \varepsilon_{33}^2) + 2e_2 E_{20}\varepsilon_{22}\varepsilon_{33}\nu_{23} + \frac{e_2 E_{20}\gamma_{23}^2}{2(1+\nu_{23})} \tag{22}$$

$$a_2 = 3 + \frac{3}{2} g_3 G_{120}(\gamma_{12}^2 + \gamma_{31}^2) + \frac{3}{2} e_3 E_{20}(\varepsilon_{22}^2 + \varepsilon_{33}^2) + 3e_3 E_{20}\varepsilon_{22}\varepsilon_{33}\nu_{23} + \frac{3}{4}\frac{e_3 E_{20}\gamma_{23}^2}{(1+\nu_{23})} \tag{23}$$

Excerpt from ISBN 978-3-00-053387-7

$$a_3 = 2g_4G_{120}(\gamma_{12}^2 + \gamma_{31}^2) + 2e_4E_{20}(\varepsilon_{22}^2 + \varepsilon_{33}^2) + 4e_4E_{20}\varepsilon_{22}\varepsilon_{33}\nu_{23} + \frac{e_4E_{20}\gamma_{23}^2}{(1+\nu_{23})} \tag{24}$$

$$a_4 = \frac{5}{2}g_5G_{120}(\gamma_{12}^2 + \gamma_{31}^2) + \frac{5}{2}e_3E_{20}(\varepsilon_{22}^2 + \varepsilon_{33}^2) + 5e_5E_{20}\varepsilon_{22}\varepsilon_{33}\nu_{23} + \frac{5}{4}\frac{e_5E_{20}\gamma_{23}^2}{(1+\nu_{23})} \tag{25}$$

The 5th order polynomial for S_r in Eq (20) is solved by the method in [18]. The solutions contain both complex numbers and real numbers and the complex numbers are excluded from being used as values for the reduced internal state variable, S_r.

4. Experiment

4.1. Characterizing internal state variable from Compressive tests

A compressive test is conducted where load is applied in the transverse direction of unidirectional composites to establish the relation between the transverse modulus and the internal state variable. A compressive test is conducted in [45] composites to to establish the relation between the shear modulus and the internal state variable. Compressive tests were performed on a servo-hydraulic universal test machine by Shimadzu Inc. An image of the experimental setup is shown in Figure 3

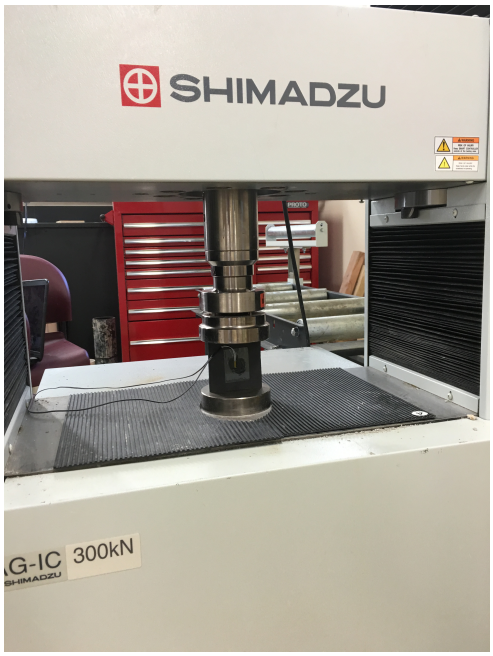

Figure 3. Setup of compression test

The width of the specimen is 71.15 mm and the height of the specimen is 71.26 mm. The thickness of the specimens ranges from 7.8 mm. For each experiment, two strain gages were attached to the specimen

Excerpt from ISBN 978-3-00-053387-7

(back to back) aligned with the loading direction and one in the transverse direction on one side. The purpose of using two strain gages in the loading direction is to monitor any unwanted bending that may occur during the compression loading. In a compressive test, A small pre-load is imposed on the specimen and all strain gages are zeroed at this state. The strain gage readings and the load cell readings are acquired at 4Hz, while the axial cross-head movement rate imposed on the specimen is 0.020 mm/sec.

The stress-strain curve for load applied in the transverse direction of composites is in Figure 4. With Figure 4, at a specific location, the corresponding internal state variable (or reduced internal state variable), S (or S_r), and degraded transverse modulus can be calculated. The coefficients for polynomial e_s related transverse modulus and reduced internal state variable are summarized in Table 1. A compressive test is conducted on a $[45]_{16}$ composite to extract the shear modulus and shear strain. The stress-strain curve for shear modulus is in Figure 5. The corresponding internal state variable (or reduced internal state variable), S (or S_r), and degraded shear modulus can be calculated. The coefficients for polynomial g_s related shear modulus and reduced internal state variable are summarized in Table 1. The plot of polynomial e_s for transverse modulus and the plot of polynomial g_s for shear modulus are in Figure 6 and Figure 7.

e_0	1	g_0	1
e_1	0.137676	g_1	-0.0837419
e_2	-0.0349585	g_2	0.00756448
e_3	0.00286427	g_3	-0.000310913
e_4	-0.000103419	g_4	5.215e-6
e_5	1.357e-6	g_5	-9.9161e-8

Table 1. The coefficients of e_i and g_i for unidirectional composites

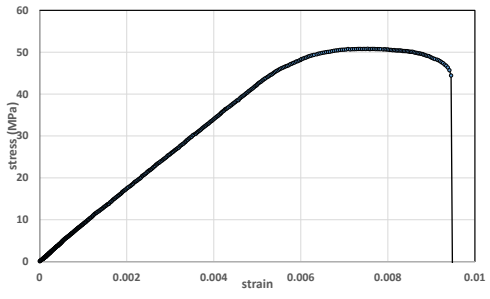

Figure 4. Stress strain curve for transverse modulus

5. Three point bending tests and simulations

The material parameters extracted from the coupon tests are implemented in 3D Schapery's theory for predicting unidirectional composites under three point bending tests. The composites plate of dimension 147.5 mm by 120 mm by 6.2 mm and the setup of the three point bending test is in Figure 8. The 3D extension of Schaperys theory for unidirectional composites is implemented in a UMAT user defined subroutine in Abaqus[19]. The stress-strain curves used in simulations for E_2 and G_{12} are in Figure 4 and Figure 5. These stress-strain curves exhibit post-peak strain softening. It has been well documented that numerical simulations utilizing constitutive laws exhibiting post-peak strain softening suffer from pathological mesh dependence [20]. It should be noted that Schaperys theory has previously been enhanced

Excerpt from ISBN 978-3-00-053387-7

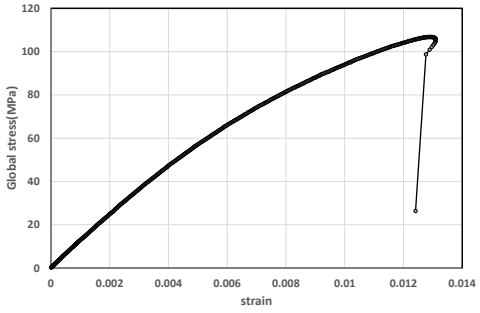

Figure 5. Stress strain curve for shear modulus

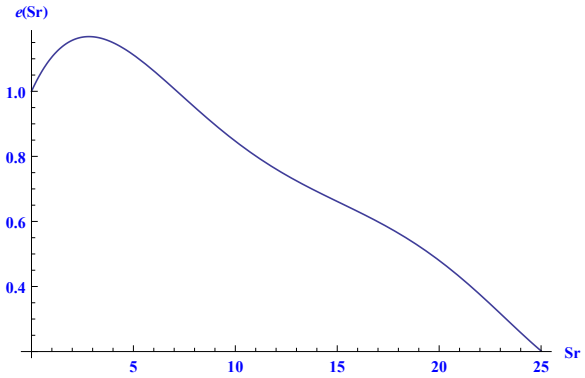

Figure 6. e_s as a function of reduced state variable S_r

to eliminate pathological mesh dependence through regularization of the energy dissipated in the post-peak regime via introduction of a characteristic element length and additional internal state variables[6]. However, that formulation is omitted herein to focus on extension of only the microdamage model to 3D.

The unloading path at any point on the stress-strain curve is assumed to follow a line connecting the current point and the origin (secant). Thus, the transverse stiffness and shear stiffness, as a function of the internal state variable S, can be calculated.

$S_r = S^{\frac{1}{3}}$ is used following [15] [6], as a reduced internal state variable for $e_S(S_r)$ and $g_S(S_r)$ in Figure 6 and Figure 7. In each step during the simulations, an incremental strain is given, and with the information given above, the corresponding S_r at this step can be calculated from Eq (20). The transverse modulus and shear modulus can then be calculated with Eq (18) and Eq (19) with the coefficients in Table 1 and used to update the integration point stresses, satisfying equilibrium. The comparison of simulations with four tests are in Figure 9. The simulations and experimental results show good agrement before the failure occurs.

6. Conclusions

In this paper, 3D Schaper's theory for unidirectional composites is used to model unidirectional composites under three point bending. Compressive tests are conducted to obtain the relation between the internal state variable and the transverse modulus, shear modulus. The simulations and experimental results show good agrement before the failure occurs.

Excerpt from ISBN 978-3-00-053387-7

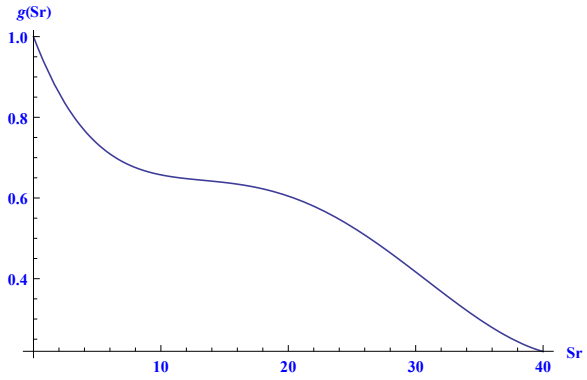

Figure 7. g_s as a function of reduced state variable S_r

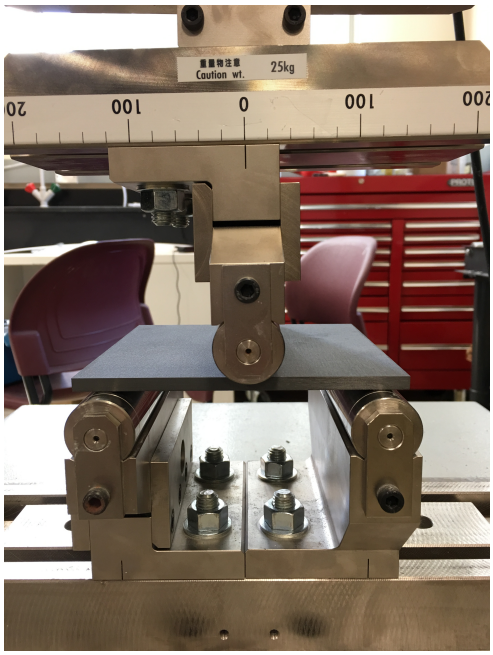

Figure 8. Setup of for three point bending

Excerpt from ISBN 978-3-00-053387-7

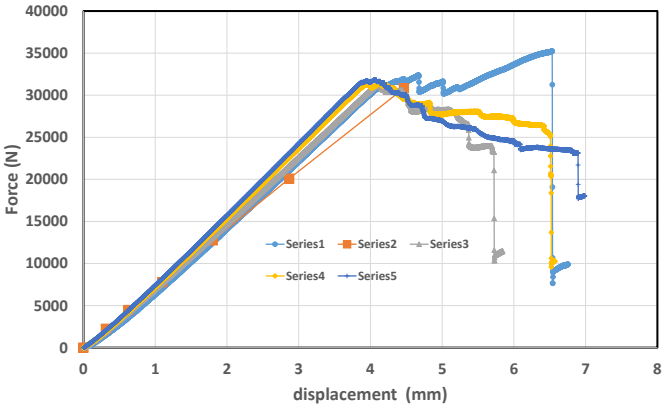

Figure 9. Comparison of simulations with test data of three point bending

Excerpt from ISBN 978-3-00-053387-7

References

[1] Tsai, S. W. and Wu, E. M. . A general theory of strength for anisotropic materials. journal of composite materials. *Journal of Composite Materials*, 5:58–88, 1971.

[2] M.A. Crisfield, Y. Mi, G.A.O. Davies . Progressive delamination using interface elements. *Journal of Composite Materials*, 32(14):1247–1271, 1998.

[3] M.D. Olsson, R. Varizi, D.L. Anderson. Damage in composites: a plasticity approach. *Journal of Composite Materials*, 44:103C116, 1992.

[4] P. Ladeveze, E. Le Dantec. Damage modelling of the elementary ply for laminated composites. *Compos Sci Technol*, 43:257C267, 1992.

[5] V.K. Williams, R. Varizi, A. Poursartip. A physically based continuum damage mechanics model for thin laminated composite structures. *Int J Solids Struct*, 40:2267C2300, 2003.

[6] Pineda, E. J., A. M. Waas. Numerical implementation of a multiple-isv thermodynamically-based work potential theory for modeling progressive damage and failure in fiber-reinforced laminates. *Int. J. Fract.*, 182:93–122, 2013.

[7] Basu, S., A. M. Waas, D. R. Ambur. Compressive failure of fiber composites under multiaxial loading. *J. Mech. Phys. Solids*, 54(3):611–634, 2006.

[8] Pineda, E. J., A. M. Waas, B. A. Bednarcyk, C. S. Collier, P. W. Yarrington. Progressive damage and failure modeling in notched laminated fiber reinforced composites. *Int. J. Fract.*, 158:125–143, 2009.

[9] Chou, T. W. *Microstructural design of fiber composites*, 1992.

[10] Tong, L., Mouritz, A.P., Bannister, M. *3D Fibre Reinforced Polymer Composites*, 2002.

[11] Ashwill TD, Veers PS, Locke J, Contreras I, Griffin D, and Zuteck MD . Concepts for adaptive wind turbine blades. *ASME 2002 Wind Energy Symposium*, Paper No. WIND2002-28:56–69, 2002.

[12] Golzar M,Poorzeinolabedin M . Prototype fabrication of a composite automobile body based on integrated structure. *The International Journal of Advanced Manufacturing Technology*, 49:1037–1045, 2010.

[13] C. R. Cater, X. Xiao, R. K. Goldberg, L. W. Kohlman. Improved subcell model for the prediction of braided composite response. *NASA/TM-2013-217875*.

[14] B. A. Bednarcyk, B. Stier, J.-W. Simon, S. Reese., E. J. Pineda. Meso- and micro-scale modeling of damage in plain weave composites. *Composite Structures*, 121:258–270, 2015.

[15] Lamborn, M. J., R. A. Schapery. A theory of mchanical behaviour of elastic media with growing damage and other changes in structure. *J. Mech. Phys. Solids*, 38(2):1725–1797, 1990.

[16] Sicking, D. L. Mechanical characterization of nonlinear laminated composites with transverse crack growth. *PhD thesis Texas AM University College Station TX*, 1992.

[17] H. Sam Huang, Evan J. Pineda. On the influence of matrix microdamage functions on the progressive failure of unidirectional composites.

[18] Skowron , Gould . General complex polynomial root solver and its further optimization for binary microlenses. *arXiv:1203.1034*, 2012.

Excerpt from ISBN 978-3-00-053387-7

[19] 2013 Users Manual, version 6.13, Dassault Systmes.

[20] Bazant, Zdenek P.; Luigi Cedolin. *Stability of Structures: Elastic, Inelastic, Fracture, and Damage Theories).* Oxford, 1991.

Excerpt from ISBN 978-3-00-053387-7